International Journal of Earth, Energy and Environmental Sciences
ISSN: 2517-942X
Vol:8, No:10, 2014

Water Depth and Optical Attenuation Characteristics of Natural Water Reservoirs nearby Kolkata City Assessed from Hyperion Hyperspectral and LISS-3 Multispectral Images

Barun Raychaudhuri

***Abstract*—**A methodology is proposed for estimating the optical attenuation and proportional depth variation of shallow inland water. The process is demonstrated with EO-1 Hyperion hyperspectral and IRS-P6 LISS-3 multispectral images of Kolkata city nearby area centered around 22º33′ N 88º26′ E. The attenuation coefficient of water was found to change with fine resolution of wavebands and in presence of suspended organic matter in water.

***Keywords*—**Hyperion, hyperspectral, Kolkata, water depth.

I. Introduction

OPTICAL reflection from the bottom surface of shallow waterbody (e.g. < 10 m) serves as an efficient tool for the estimation of its depth, which may be important for the sake of bottom topography [1], assessment of sediment concentration [2] and natural resources [3] and many other aspects. It is also expected to facilitate human activities, such as water level monitoring in barrages and fisheries.

The basic principle of optical bathymetry is to compare the radiation reflected from different depths of bottom surface. Generally two types of techniques are in use. One group uses a single satellite image and compares that with truth depth data procured from ground [4], [5]. The other method is to compare two or more images of the same spot acquired at different times [6]. Both field-based and airborne measurements are reported [2]. Moderate spatial resolution multispectral satellite images like LANDSAT [4], SPOT [6] and IRS [7] are widely used. Along with these optical methods, other techniques, such as radar interferometry [8] are also adopted for bathymetry. Hyperspectral data are relatively less applied to water depth studies. However, bathymetry of coastal regions using Hyperion images [9], [10] and atmospheric correction to similar studies [11] are reported. Hyperspectral satellite images in connection with inland water depth estimation are not so widely used as yet.

The present work carries out the assessment of depth and optical attenuation for shallow inland water by optical reflection technique using Hyperion hyperspectral and LISS-3 multispectral images. Generally green wavebands are preferred for optical bathymetry because of large penetration depth [6], [7]. The present work has studied the effect of both green and red wavebands on the optical attenuation for varying water depth. Changes have been noticed for finer spectral resolutions and in presence of suspended organic matter in water.

Barun Raychaudhuri is with Department of Physics, Presidency University, 86/1 College Street, Kolkata 700073, India (e-mail: barun.raychaudhuri@gmail.com).

Financial support is provided by the institution.

II. Materials and Methods

The work comprises the analysis of EO-1 Hyperion hyperspectral and IRS P6 LISS-3 multispectral images of an area centered around 22º33′ N 88º26′ E near Kolkata city. Some relevant properties of the two sensors are mentioned in Table I. Both have the same spatial resolution. The Hyperion image was downloaded from USGS website and its green and red bands were chosen so as to match the corresponding LISS-3 bands.

TABLE I
Comparison of Hyperion and Liss-3 Sensors

Parameter	Hyperion		LISS-3
Pixel resolution	30 m		30 m
Spectral resolution	10 nm		70 nm, 60 nm
Green wavebands	Band name	Central wavelength (nm)	520-590 nm
	Band-17	518.39	
	Band-18	528.57	
	Band-19	538.74	
	Band-20	548.92	
	Band-21	559.09	
	Band-22	569.27	
	Band-23	579.45	
Red wavebands	Band-27	620.15	620-680 nm
	Band-28	630.32	
	Band-29	640.50	
	Band-30	650.67	
	Band-31	660.85	
	Band-32	671.02	
	Band-33	681.20	

A specific area within the satellite images comprises a large assemblage of pond-like natural water reservoirs. The distribution of waterbodies and their extension are indicated in Figs. 1 (a) and (b). A number of small zones within these water reservoirs, expected to have varying water depths were chosen at random using ENVI 4.7 software, a few being indicated by numbers in Fig. 1 (a). The approximate surface areas of two such ponds, estimated by counting the number of

pixels, are shown as example in Fig. 1 (b). Each chosen small zone of varying depth consisted of 50 to 100 pixels. The DN values for each zone corresponding to each green (17 to 23) and red (27 to 33) band were averaged over the pixels and divided by the prescribed scaling factor of 40 to obtain the average radiance value ($Wm^{-2}sr^{-1}\mu m^{-1}$) over that zone. A similar process was repeated for the single, wide green and red bands of LISS-3 image. These average radiance values were utilized to derive information on water depth and bottom albedo using the following theory.

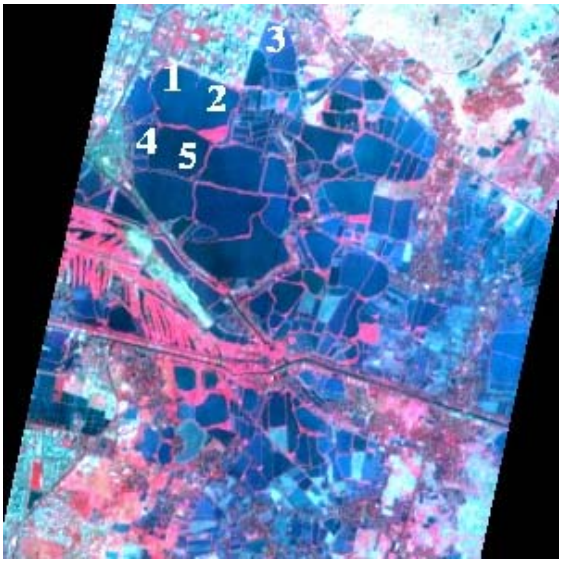

(a)

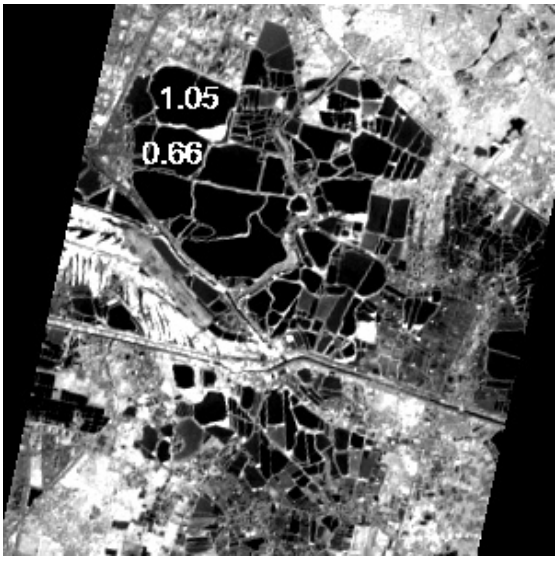

(b)

Fig. 1 Hyperion image of January, 2010 showing the distribution of natural water reservoirs: (a) FCC [Bands 42+ 32+21] indicating few randomly chosen regions of varying water depth (b) same image in Band-42 indicating approximate surface areas of two such reservoirs

Assuming the radiation attenuation through the water following Lambert-Beer law, the upwelling radiance (L_z) from water surface, measured from above for an arbitrary water depth (z) can be expressed as a linear combination of the radiance component reflected from the bottom surface and that reflected from the depth of the waterbody so that

$$L_z = TL_B + (1-T)L_w \,, \tag{1}$$

where

$$T = \exp(-kz) \tag{2}$$

is the transmittance of the water, k being its attenuation coefficient, a constant for certain wavelength of radiation. L_B is the bottom radiance and L_w is the deep water radiance. Combining (1) and (2),

$$L_z = L_w + (L_B - L_w)\exp(-kz) \,, \tag{3}$$

which indicates that for very shallow water, $z \approx 0$ and the measured radiance is dominated by the bottom albedo. When the water is very deep, $z \approx \infty$ and the bottom radiance becomes negligible. In between, the change in radiance measured at the sensor occurs due to the variation of both water depth and bottom properties. For a finite region having similar type of bottom soil, L_B and L_w are constant quantities and the change in L_z is caused by the varying depth (z) of water, which is obtained from (3) as

$$z = \frac{1}{k}\ln\frac{L_B - L_w}{L_z - L_w} \tag{4}$$

For two different depths z_1 and z_2 of two locations of the same image having measured radiance values L_{z1} and L_{z2}, respectively,

$$\ln\frac{L_{z2} - L_w}{L_{z1} - L_w} = k(z_1 - z_2) \,, \tag{5}$$

which can also be obtained by differentiating (3) with respect to depth and integrating the quantity $dL_z/(L_z - L_w)$ between the limits L_{z1} and L_{z2}.

III. Results and Discussion

Since L_B and L_w in (4) are constant quantities having some fixed values for a certain waveband, the plot of radiance values of the i-th band against that of the j-th band for the same depth is expected to yield the value of k_j/k_i as the slope. Figs. 2 (a) & (b) show two examples of such plots for different green bands of the Hyperion image. The straight lines indicate uniformity in bottom radiance, hence uniform bottom surface property over the region. The k values for water for different green and red bands thus obtained are compiled in Table II. Slight changes in k values are noted over the entire green and red wavelength ranges and the change is opposite in green and red regions.

The LISS-3 images having the same spatial resolution as

above and covering the above mentioned entire green and red wavelength ranges within single bands are, therefore expected to produce the average effect of optical attenuation, bottom surface property and effect of suspended matter. Two such images of the same region consisting of the same group of water reservoirs are shown in Figs. 3 (a) and (b).

TABLE II
COMPARISON OF K-VALUE RATIOS FOR HYPERION GREEN AND RED BANDS

Bands plotted	*k*-ratio	Bands plotted	*k*-ratio
Band-18 vs. Band-17	1.098	Band-28 vs. Band-27	0.9349
Band-19vs. Band-17	1.134	Band-29vs. Band-27	0.9179
Band-20vs. Band-17	1.198	Band-30vs. Band-27	0.9078
Band-21 vs. Band-17	1.233	Band-31 vs. Band-27	0.8052
Band-22vs. Band-17	1.219	Band-32vs. Band-27	0.7904
Band-23vs. Band-17	1.156	Band-33vs. Band-27	0.7461

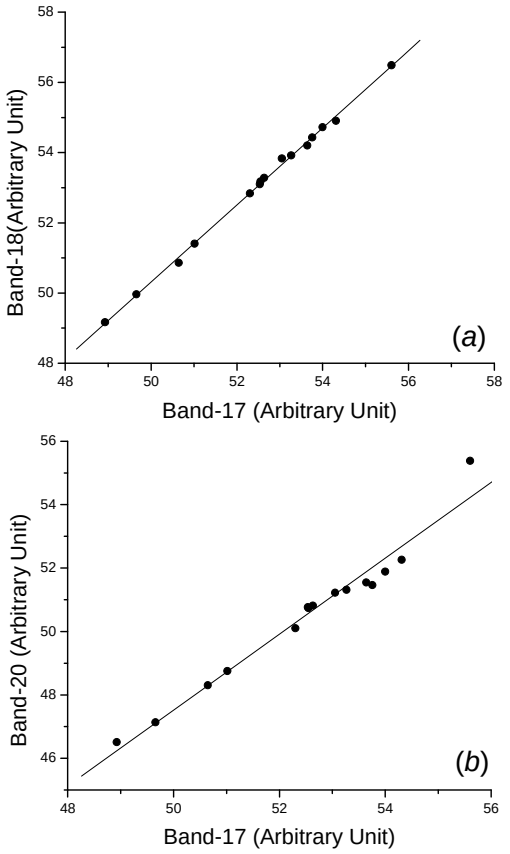

Fig. 2 Plots of (a) Band-17 vs. Band-18 and (b) Band-17 vs. Band-20 of Hyperion image to showing the change in *k* ratio with wavelength (b) same image in Band-42 indicating approximate surface areas of two such reservoirs

Fig. 3 (a) is contemporary to the Hyperion image of Fig. 1 and Fig. 3 (b) is of one decade ago. The wide time gap is expected to change the physical properties of the region. Both images are shown in green band. The abundance of suspended organic matter like algae is larger in the 1999 image, as apparent from larger green radiance. The plots of radiance values of green and red bands for these two images are shown in Figs. 4 (a) and (b), which exhibit change in *k*-ratio, as mentioned within the figures.

(a)

(b)

Fig. 3 LISS-3 image in green band of the same region as that in Fig. 1 for: (a) March, 2009 and (b) March, 1999

Since the bottom reflectance remains more or less unchanged for the regions under consideration, (5) can be simplified further as follows. Replacing the quantity $(L_z - L_w)$ in denominator by the minimum measured radiance (L_{min}), which corresponds to the maximum depth (z_{max}) under the random sampling, the ratio of L_{min} to the measured radiance for other depths can be expressed as

$$\ln(L_z / L_{min}) = k(z - z_{max}). \quad (6)$$

It shifts the ratio by a constant term but keeps the nature of

variation unchanged. Equation (6) has both k and $(z - z_{max})$ as unknown quantities and cannot be determined explicitly. However, for moderate change in depth, k may be assumed to be constant. In that case the ratio of the quantity $\ln(L_z/L_{min})$ for two depths with respect to the same maximum depth can express a ratio proportional to the two depths. This assumption is not valid for large depth because then the bottom properties become negligible.

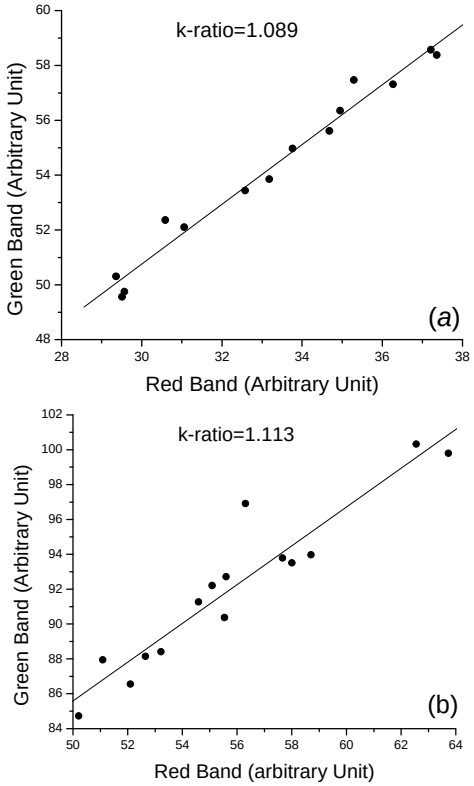

Fig. 4 Band plots for LISS-3 images of (a) March, 2009 and (b) March, 1999 showing the change in k ratio

TABLE III
COMPARISON OF PROPORTIONAL DEPTH RATIOS WITH RESPECT TO THE MINIMUM, AS OBTAINED FROM HYPERION AND LISS-3 GREEN AND RED BANDS

Hyperion		LISS-3, 2009		LISS-3, 1999	
Band-17	Band-27	Green	Red	Green	Red
2.51	2.71	3.34	4.53	2.27	2.63
1.58	2.28	3.28	4.61	2.20	2.85
1.80	2.21	2.96	3.49	1.81	1.37
1.52	1.73	2.91	4.03	1.39	1.87
1.32	1.60	2.57	3.3	1.33	1.73
1.52	1.44	2.3	3.15	1.21	1.22
		2.07	2.62	1.14	1.11
		1.66	2.29		
		1.51	1.93		

Following the above concept, the radiance values for randomly sampled zones were arranged in descending order, the maximum and minimum value representing the minimum and maximum depth, respectively among the samples. The proportional depth ratios calculated for different zones from the Hyperion and LISS-3 images are shown in Table III. Though there is fluctuation, the values lie within a certain limit.

IV. CONCLUSION

A methodology is proposed for assessing the depth and optical attenuation for shallow inland water by optical reflection technique solely based on satellite image analysis without ground measurement. The method was validated with EO-1 Hyperion hyperspectral and IRS-P6 LISS-3 multispectral images for natural water reservoirs centered around 22º33′ N 88º26′ E nearby Kolkata city. The attenuation coefficient of water was found to change with fine resolution of both red and green wavebands and also in presence of suspended organic matter in water. Though the depth could not be estimated directly, a qualitative assessment of proportional depth variation could be obtained for randomly sampled zones within the image.

REFERENCES

[1] C. D. Mobley, and L. K. Sundman, "Effects of optically shallow bottoms on upwelling radiances: Inhomogeneous and sloping bottoms", *Limnology and Oceanography*, vol.48, pp. 329–336, 2003.
[2] C. J. Legleiter, D. A. Roberts, and R. L. Lawrence, "Spectrally based remote sensing of river bathymetry", *Earth Surface Processes and Landforms*, vol. 34, pp. 1039–1059, 2009.
[3] E. J. Hochberg, M. J. Atkinson, and S. Andrefouet, "Spectral reflectance of coral reef bottom-types worldwide and implications for coral reef remote sensing", *Remote Sensing of Environment*, vol. 85, pp. 159–173, 2003.
[4] M. Ibrahim, and A. P. Cracknell, "Bathymetry using Landsat MSS data of Penang Island in Malaysia", *International Journal of Remote Sensing*, vol. 11, pp. 557–559, 1990.
[5] S. Bagheri, M. Stein, and R. Dios, "Utility of hyperspectral data for bathymetric mapping in a turbid estuary",*International Journal of Remote Sensing*, vol. 19, pp. 1179–1188, 1998.
[6] H. M. Kao, H. Ren, C. S. Lee, C. P. Chang, J. Y. Yen, and T. H. Lin, "Determination of shallow water depth using optical satellite images", *International Journal of Remote Sensing*, vol. 30, pp. 6241–6260, 2009.
[7] N. K. Tripathi, and A. M. Rao, "Bathymetry mapping in Kakinada Bay, India, using IRS-1D LISS-III data", *International Journal of Remote Sensing*, vol. 23, pp. 1013–1025, 2002.
[8] M. Durand, E. Rodriguez, D. E. Alsdorf, and M. Trigg, "Estimating river depth from remote sensing swath interferometry measurements of river height, slope, and width", *IEEE Journal of Selected Topics in Applied Earth Observations and Remote Sensing*, vol. 3, pp. 20–31, 2010.
[9] Z. P. Lee, B. Casey, R. Parsons, W. Goode, A. Weidemann, and R. Arnone, "Bathymetry of shallow coastal regions derived from space-borne hyperspectral sensor", Proceedings of Ocean 2005 MTS/IEEE Conference & Exhibition, Washington D.C., USA, 18-23 September, 2005.
[10] L. Zhang, B. Zhang, Z. Chen, L. Zheng, and Q. Tong, "The application of hyperspectral remote sensing to coast environment investigation", *Acta Oceanologica Sinica*, vol. 28, pp. 1–13, 2009.
[11] Z.Liu, and Y. Zhou, "Direct inversion of shallow-water bathymetry from EO-1 hyperspectral remote sensing data", *Chinese Optics Letters*, vol. 9, pp. 060102-1–4, 2011.